Journal of Polymers and the Environment (2020) 28:1150–1159
https://doi.org/10.1007/s10924-020-01672-4

ORIGINAL PAPER

A New Proposal of Preparation of Different Polymorphs of Nanocellulose from *Eucalyptus citriodora*

Alana G. de Souza[1] · Mariana T. Junqueira[1] · Giovanni F. de Lima[1] · Vijaya K. Rangari[2] · Derval S. Rosa[1]

Published online: 6 February 2020

Abstract

Cellulose is a renewable, sustainable, and high available biopolymer; their common form is the type-I polymorph. However, polymorphic changes are associated with different properties and a wide range of applications. In this study, we proposed a new method to prepare polymorphic cellulose nanostructures (CNSs): first, the CNS were isolated, and then the polymorphs were converted. CNS-I (type-I), CNS-II (type-II), and CNS-III (type-III) were successfully obtained, and the structure, crystallinity, superficial characteristic, morphology, and thermal stability were evaluated. The results showed that CNS-II and CNS-III are more amorphous than CNS-I due to the strong reagents used for the polymorphic conversion, which results in a swelling, increased chain spacing, and structural disorganization. This effectively changed the morphology of the CNS, from cellulose nanocrystals from irregular quasi-spherical nanoparticles. The proposed method allows a wide range of applications, from package and nanocomposites with CNS-I due to its high crystallinity and crystal morphology, to drug carrier, food thickener and biomedical products for CNS-II and CNS-III due to its quasi-spherical shape and more amorphous structure.

Keywords Cellulosic polymorphs · Cellulose nanostructures · Eucalyptus residues · Biomass valorization

Introduction

Cellulose is a biodegradable, sustainable, renewable, and abundant biopolymer. Agricultural, forest, and industrial wastes may be used to prepare cellulose and isolating their nanostructures (CNSs) due to its availability and low cost. Eucalyptus waste is an attractive raw material due to its high content of cellulose (~ 35 wt%) and good mechanical and thermal properties [1–3]. The revalorization of these forest byproducts is a way to make the production of sustainable and renewable materials more commercially attractive.

The eucalyptus sawdust has in its composition native cellulose, mainly cellulose I_β (monoclinic two-chain unit cell—parallel chains) [4]. However, cellulose has more than one polymorphic structure, that is, different dimensions can be found for the unit cell (identified as type I, II, III and IV); and the cellulose-I is the basic crystalline structure that is found in a wide variety of cellulosic fibers.

The properties and physicochemical characteristics of each polymorph are different (i.e., hydrophobicity, oil/water interface, mechanical properties, the morphology of the particle, and others), which allows different applications. Cellulose type I can be used for the synthesis of hydrogels and as reinforcement to improve mechanical properties; the type II is a bioethanol feedstock and can be used to prepare pharmaceutical tablets; and type III, due to its amorphous nature, can be used as emulsion stabilizer (for example, in Pickering emulsions) [5].

Cellulose type II is an amorphous structure with a bigger space between the chains and more hydrogen bonds than the native form; it is obtained from an irreversible transformation of cellulose I by mercerization or regeneration [4]. Cellulose type III is obtained from treating one of the previous polymorphs (I or II) with liquid ammonia in low temperatures or organic amines, such as ethylenediamine (EDA), and the transformation is reversible; the result is the decrystallization and fragmentation of the crystals [4]. The

Electronic supplementary material The online version of this article (https://doi.org/10.1007/s10924-020-01672-4) contains supplementary material, which is available to authorized users.

✉ Derval S. Rosa
dervalrosa@yahoo.com.br

[1] Engineering, Modeling and Applied Social Sciences Center (CECS), Federal University of ABC, Avenida dos Estados, 5001, Santo André, SP CEP: 09210-580, Brazil

[2] Department of Materials Science and Engineering, Tuskegee University, Tuskegee, AL 36088, USA

last polymorph is cellulose IV, obtained by high-temperature treatment of cellulose III [4]. However, its existence is questioned by some researchers since it has characteristics very similar to cellulose I [4, 6].

Considering the importance of the development of sustainable materials for reducing environmental impacts as the inadequate disposal of eucalyptus, the preparation of cellulose nanostructures is an excellent alternative. The advantages of the CNS are the possibility of being isolated from a wide range of sources, the different routes of production and the less environmental harming manufacturing when compared to other carbon sourced products [7, 8]. Currently, the researches of this material are focused on the development of nanocomposites, membranes for water filtration, drug delivery capsules, and packaging application [9].

Typical isolation processes can be employed to prepare CNS, and the acid hydrolysis is the most common. However, due to the increasing concerns related to production and excessive consumption of disposable plastic products and the consequents environmental impacts of plastic pollution, is there an increasing search for sustainable alternatives. The ball mill is considered an environmentally friendly route, with no chemical byproducts, that is a potential substitute for the chemical routes [10]. Concerning the obtention of different CNS polymorphs, the literature has a few works that involve two steps: the first one is the obtention of the cellulosic polymorphs; the second is the conversion of micro into nanocellulose, as presented by Gong et al. (2018) and Mahmud et al. (2019) [5, 11]. To obtain the different polymorphs in the form of nanoparticles, the literature has a well-established sequence: first, the conversion of type I cellulose into its polymorphs; later, the polymorph is transformed into nanocellulose. However, the preparation of the polymorphs before isolation is a challenge that has a strong influence on several parameters, such as shapes, sizes, thermal stability, and others. These nanoparticles can be applied in biodegradable polymers to improve the mechanical and thermal properties, aiming a revolution of the packaging industry due to its versatility, lightness, easy processing, and durability.

The literature presents some works that perform the transformation of cellulose into its polymorphs and subsequent transformation into nanocellulose [11–14]. In the present work, it was investigated the conversion of eucalyptus biomass into nanocellulose, and later the polymorphic transformation, evaluating its impacts on the physicochemical properties of the nanostructure. Our proposal was present a conversion approach not presented in the literature yet, first converting the eucalyptus into nanocellulose by ball mill, and after preparing the cellulose polymorphs. Also, we investigated the relationship between the CNS morphology and the chemical structure arrangement. This work aims to obtain nanoparticles with different properties, which allow the valorization of this forest byproduct and increase the applicability of the prepared CNS.

Experimental Section

Materials

The raw material was Eucalyptus residues (*Eucalyptus citriodora*) (*ER*) obtained after harvesting and cutting in Mato Grosso (Brazil). This raw material had a composition of ~ 33% of cellulose, ~ 27% of hemicellulose and ~ 33% of lignin. All the reagents were obtained from Labsynth (SP, Brazil).

Production of Cellulose Nanostructures (CNSs)

Two chemical treatments were performed for removing non-cellulosic components (lignin and hemicellulose). In the first treatment (*T1*), the ER was treated with sodium chlorite solution—$NaClO_2$ (3.9 wt%) for 2 h at 70 °C under mechanical stirring; then the samples were washed until neutral pH and dried at 50 °C for 12 h, obtaining a yield of 60% and a material with 61% of cellulose, 20% of hemicellulose and 14% of lignin.

The T1 sample was submitted to the second treatment (*T2*) with potassium hydroxide—KOH (10 wt%) and sodium hydroxide—NaOH (10 wt%) for 2 h at room temperature under mechanical stirring; then, the was washed until neutralization and dried at 50 °C for 12 h. At the end of the second treatment, the yield was ~ 40 wt% (compared with the initial mass of dried samples), and the final material presented ~ 93% of cellulose, ~ 2% of hemicellulose and ~ 5% of lignin.

To isolate the cellulose nanostructures (CNSs), the T2 sample was mixed to ethanol (80 wt%) (proportion 1:1), and submitted to grinding in ball milling (Marconi, MA500) for 12 h, with alumina balls in the weight ratio 1:80 (sample/balls). The result of the grinding is native CNS (named *CNS-I*).

To obtain the polymorphs, the following treatments were used to promote structural changes starting from CNS-I. *Cellulose type II* the CNS-I was mixed with NaOH solution (18.5 wt%) for 24 h at room temperature under mechanical stirring. The solution was dialyzed in membrane until neutralization (*CNS-II*). *Cellulose type III* the CNS-I was treated with ethylenediamine (EDA) for 24 h at room temperature, using the ratio 1 g of CNS to 25 mL of solution. Then the sample was washed with ethanol. The sample was dialyzed in membrane until neutralization (*CNS-III*).

Characterization

FTIR spectra of the samples were recorded on a Frontier 94942 (PerkinElmer, USA) in the range of 400–4000 cm^{-1}, resolution 2 cm^{-1} and 64 scans. The energy of the hydrogen bonds was calculated according to the Eq. 1, where ν_0 is the standard frequency of –OH groups (cm^{-1}), ν is the frequency of –OH groups (cm^{-1}), $K = 1.6 \times 10^{-2}$ $kcal^{-1}$ [15].

$$E_H = \frac{1}{K} \times \frac{\nu_0 - \nu}{\nu_0}. \quad (1)$$

The X-ray diffraction patterns were obtained on a STADI-P (Stoe), operating in transmission mode, with Cu Kα radiation (λ = 1.54056 Å), selected by a curve monochromator of Ge (111), using a range from 0° to 60°, with a pace of 0.06°. The crystallinity index (CI) was calculated using Eqs. 2 and 3 [16, 17]:

$$CI_{\text{Cellulose I}} = \frac{I_{200} - I_{18.5°}}{I_{200}}, \quad (2)$$

$$CI_{\text{Cellulose II}} = \frac{I_{110} - I_{15°}}{I_{110}}, \quad (3)$$

where I_{200} is the intensity of the crystalline 200 peak (at about 2θ = 26°), I_{110} is the peak at 2θ = 18°. The $I_{18.5}$ and I_{15} correspond to the amorphous part.

The X-ray photoelectron spectroscopy (XPS) analysis was carried out using a ThermoFisher Scientific, model K-alpha$^+$, equipped with monochromatic radiation Al Kα at room temperature operated at 10 or 20 eV for high-resolution scans. Data were treated with CASAXPS software.

The DLS analysis was used to evaluate the statistical size distribution of the CNS and was carried out using dynamic light scattering system (ALV-CGS3), with scattering light at 90°. The hydrodynamic radius was obtained through an approximation of the crystal size of a spherical particle, with CNS dispersion in water (concentration equalized to 0.01 wt%).

Zeta potential of the nanoparticles was determined by measuring electrophoretic mobility and conversing the values through the Helmholtz–Smoluchowski equation. The equipment used to characterize the surface charge property of nanoparticles was a Zetasizer Nano-ZS (Malvern Instruments).

The surface morphology of all the samples was investigated by transmission electron microscopy (TEM-Jeol 2010). A drop of the colloidal solution at 2 wt% was deposited on a copper grid for analysis.

The thermal behavior of the samples was verified on a Q500 instrument (TA Instruments), by progressive heating of 20–600 °C, a heating rate of 20 °C/min and N_2 atmosphere.

Results and Discussion

Fourier Transform Infrared Spectroscopy

The characterization of the samples after the chemical treatments (T1 and T2) is presented in the Supplementary Material of the present work. In the Supplementary Material, Table 1S is also presented, in which all characteristic peaks are assigned in detail.

FTIR spectroscopy was used to elucidate the chemical structure of the cellulose nanostructures (CNSs) and its polymorphs. The spectra of CNS-I, CNS-II, and CNS-III is presented in Fig. 1. The transformation of the polymorphs results in the different crystalline organization of the cellulosic chains, which reflect in small shifts and new shoulders [18]. However, as the chemical structure is similar, there are only slight changes in the spectra [19]. According to Kim et al. (2013), the differences between cellulose spectra of type I, II, and III are found at wavelengths less than 800 and greater than 3000 cm^{-1} [20]. The band between 3500 and 3200 cm^{-1} slightly change intensity in the spectra of the polymorphs, which represents variation in the amount of hydroxyl groups in cellulose due to the scission of hydrogen bonds.

Considering the band 3500−3200, which is relative to the hydrogen bonds, the energy E_H was calculated, and the values are presented in Fig. 1. The hydrogen bonds are stronger in the CNS-III than the CNS-II. As these bonds are associated with the cellulose crystalline domains, it is expected that the CNS-II is more amorphous than the others. Moreover, as the CNS-III presents higher amounts of hydrogen bonds between the chains, the cellulose structure becomes

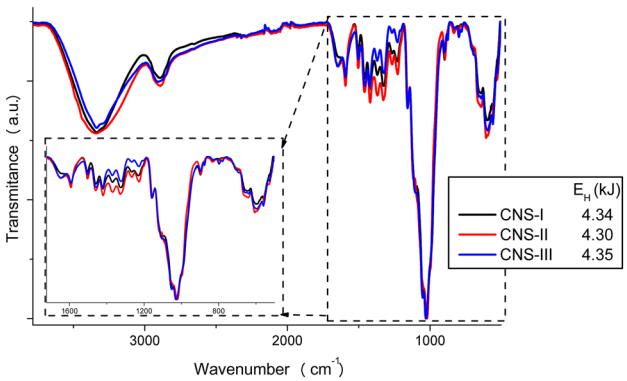

Fig. 1 Full FTIR spectra of CNS and their polymorphs, with a zoom of the region 1600−750 cm^{-1}

more packed, which should result in higher crystallinity and thermal stability [21].

Evaluating the three spectra in detail, the peaks that need to be highlighted were: 1163, 1154, 1118, 2892 cm^{-1} and the band 3400–3200 cm^{-1}; these peaks showed a slight shift in the spectrum of CNS-II and/or CNS-III, which suggests the transformation between polymorphs (Fig. 2); the peak at 895 is also indicative of cellulose type II [5, 22]. The peak 897 cm^{-1}, for CNS-I, was a broader band; for CNS-II, a sharp peak translated to smaller wavelength (895 cm^{-1}); for CNS-III, this peak was less intense and again at high wavenumber [23].

Regarding the cellulose polymorphs, Fig. 3 shows the zoom of the band 3400–3200 cm^{-1} and the peaks 1163, 1110 and 897 cm^{-1} to demonstrate the shifts and/or changes in their intensities. The shifts and intensities' changes are related to the disruption of the regularity of the crystal lattice, forming new less-organized hydrogen bonds, reflecting in the FTIR spectra. The main difference of cellulose type-I and their polymorphs involves the rotation about the glucosidic linkage caused by a disturb in the intramolecular system of the cellulose type-I [23], reflecting in small changes in the spectra of CNS-II and CNS-III.

For the CNS-II, the peaks 1163 and 1110 cm^{-1} were shifted to 1154 and 1118 cm^{-1}, respectively, which is characteristic of amorphous cellulose [23]; the peak 897 cm^{-1} is sharper for the CNS-II than for CNS-I. In the CNS-III spectra, a new band at ~870 cm^{-1} and a should at ~3280 were observed, which is indicative of a change in the crystalline structure of cellulose. CNS-III was expected to exhibit more significant variations in the spectrum. As the changes were subtle or imperceptible, there is evidence that the conversion has been partial, as discussed in the other analyzes.

This evidence confirms that the proposed method of this article is efficient in the polymorphic transformation conducted after the nanocellulose preparation.

X-Ray Diffraction

Crystallinity is an important property of nanocellulose that determines its mechanical and physical properties, and these factors have a strong influence in the final application of the nanoparticles. High crystallinity probably will be good reinforcement in nanocomposites, while low crystallinity is indicated to apply as a food thickener or Pickering emulsion, for example. The XRD patterns of CNS-I, CNS-II, and CNS-III are presented in Fig. 3a. The cellulose type-I characteristic peaks are found in $2\theta = 15°$, 16.5° and 22.5°, corresponding respectively to the planes of the crystalline lattice with Miller (1 1 0), (110) and (200); type-II peaks are found in $2\theta = 12°$, 20° and 22°, corresponding to (1 1 0), (110) and (020); type-III peaks are observed in $2\theta = 12°$ and 17° assigned to the planes (010) and (002), and 21° that comprises the planes (100), (012) and (1 1 0) [11]. The cellulose-II peaks can be easily identified, confirming the conversion of the type-I polymorph to type-II. Considering that the diffraction patterns of type I and type II pulp are very similar, it is believed, based on the other techniques associated with XRD, that type I pulp was converted to cellulose II. This is because, unlike what was observed for cellulose III, where the CNS-I peaks are clearly identifiable, this does not happen for the CNS-II diffractogram.

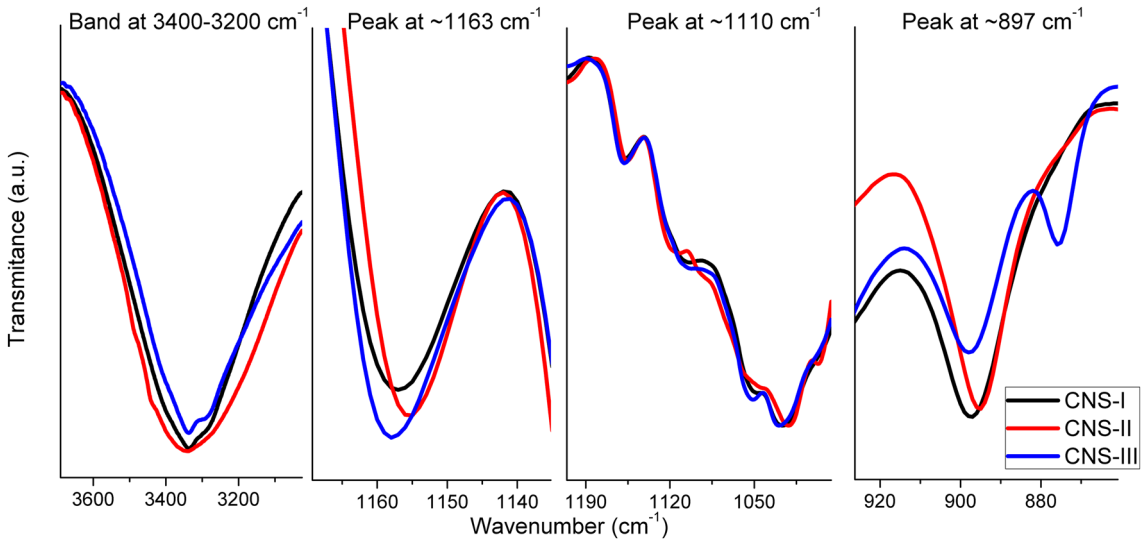

Fig. 2 Zoom of FTIR spectra: main peaks evaluated for the cellulosic polymorphs: band 3400–3200 cm^{-1} and peaks at: 1163, 1110 and 897 cm^{-1}

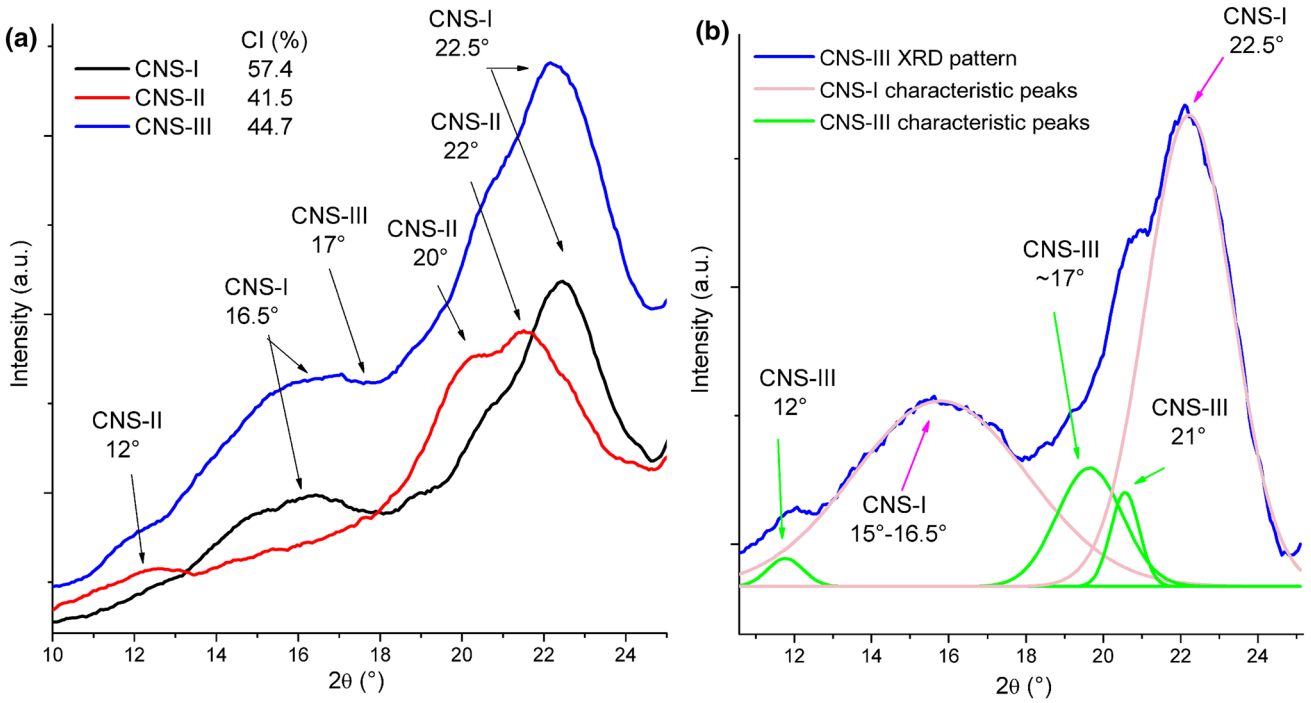

Fig. 3 **a** XRD patterns of CNS-I, CNS-II and CNS-III and the indicative of the main peaks of each polymorph and **b** deconvolution of XRD pattern of CNS-III

In the XRD pattern of CNS-III and its deconvolution, peaks associated with polymorphs I and III of cellulose can be observed in Fig. 3b. This fact, associated with the FTIR spectra, allow the conclusion that the conversion of cellulose I in cellulose III was partial. It is important to mention that the literature reports difficulties in obtaining a high conversion rate for cellulose III, even in extreme conditions, such as the use of negative temperatures [24, 25].

Regarding the crystallinity, the polymorphs II and III showed lower CI values than CNS-I. According the literature, the cellulose type-III is amorphous; as we obtained a mix of cellulose polymorphs, as identified on the XRD pattern deconvolution, the CI was calculated using the cellulose I peaks and applying the Eq. 2. The reduction in CI was 16% in the transformation to CNS-II and 13% to CNS-III, and can be associated with the use of strong reagents (EDA and concentrated NaOH); the reaction results in a greater spacing between cellulose chains, which tend to disorganize, when compared with CNS-I [13, 24].

X-Ray Photoelectron Spectroscopy (XPS)

The XPS technique is used to analyze the concentration of elements present on the surface of a sample (to the depth of 10 nm); the analysis was performed to compare oxygen:carbon ratio of the polymorphs. The full XPS spectra of CNS and its polymorphs are presented in Fig. 4a. The CNS-I presented only C and O in its composition, which is expected.

Figure 5a shows a schematic of the interaction of X-rays with the sample structure. Given the depth that the radiation can reach (10 nm), the test detects only the carbonic structure and surface hydroxyl on CNS-I, which presented an O:C ratio of ~65%.

On the surface of the sample CNS-II, the elements C, O, and Na were observed (Fig. 4b). This third element is justified by the treatment used to convert cellulose-I in cellulose-II (NaOH solution). In this process, the Na^+ ion extends the accessible regions between the crystallographic planes of the cellulosic structure to allow the Na^+ ions to diffuse between these planes. Intermediate structures were then formed, called alkaline cellulose-I and alkaline cellulose-II. The first intermediate structure is formed in the amorphous region and maintains a relatively large distance between the cellulose chains, since the –OH groups are replaced by O–Na groups [13]. If the NaOH concentration is high enough, the crystalline areas of cellulose-I begin to transform into alkaline cellulose II. After dialysis, the Na^+ ions were partially removed, and the type II cellulose structure was obtained. The expected structure is presented in Fig. 5b. For this sample, O:C ratio was ~54%.

The CNS-III presented C, O, and N in its surface (Fig. 4d). The nitrogen atoms are remnants of the reaction

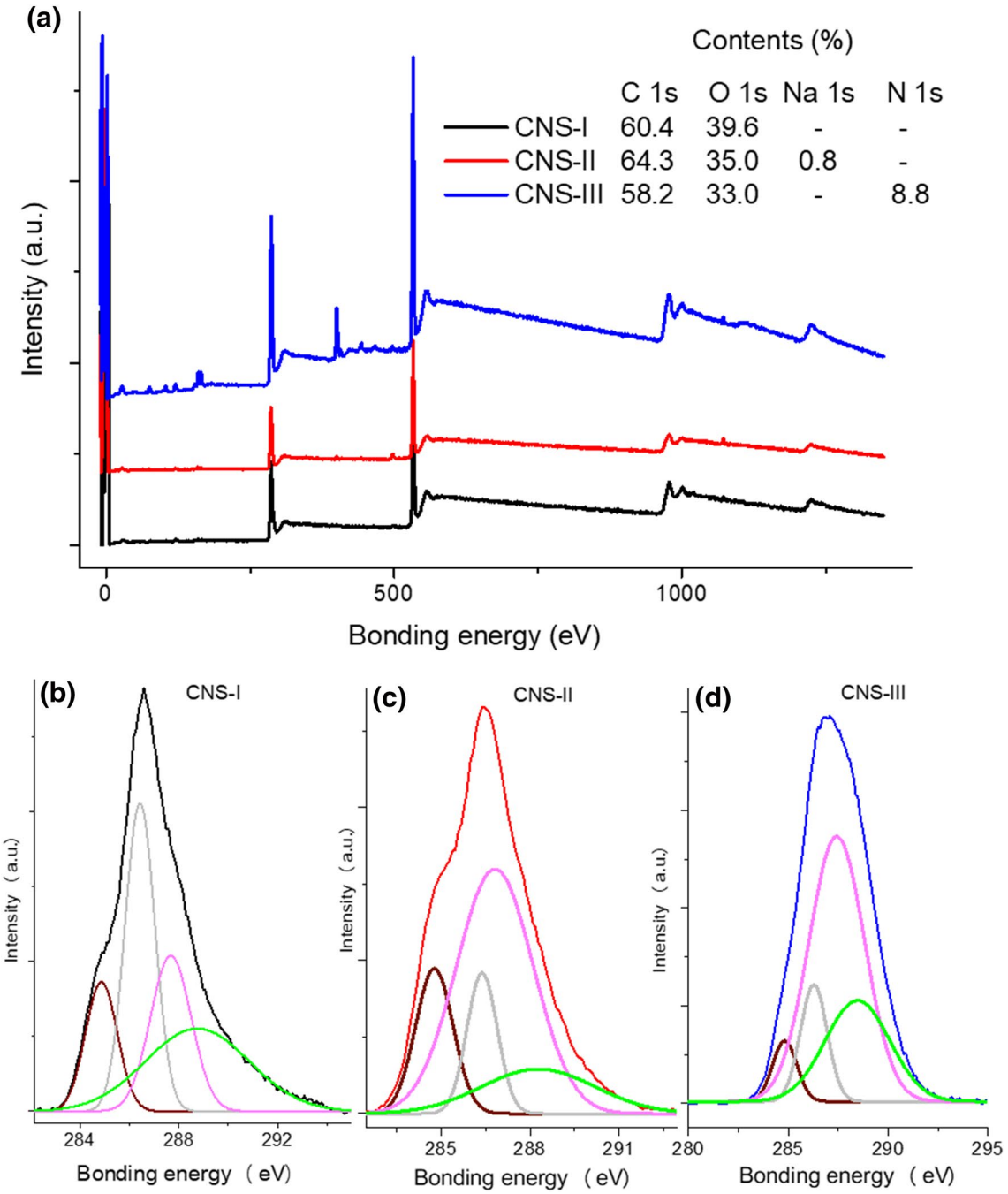

Fig. 4 **a** Full XPS spectra of CNS and their polymorphs; and C 1s XPS spectra of **b** CNS-I, **c** CNS-II and **d** CNS-III

with EDA. It was observed that the reduction in the concentration of O atoms corresponds to a similar amount that increases the nitrogen content, which can be justified by the replace of free oxygen (hydroxyls) to nitrogen. Even after sample neutralization and dialysis, nitrogen remained on the surface of the material, which is indicative of a structural change caused by EDA (Fig. 5c).

Dimensional, Stability, and Morphological Analysis

Evaluating the DLS results, it was observed that the average size of CNS-I was around 90 nm (Fig. 5d). CNS-II presents bimodal distribution, with peaks at 350 and 450 nm. The increase of the average size from CNS-I to CNS-II may be justified by the effect of swelling of the fibers during mercerization [13]. Broader size distribution was observed in

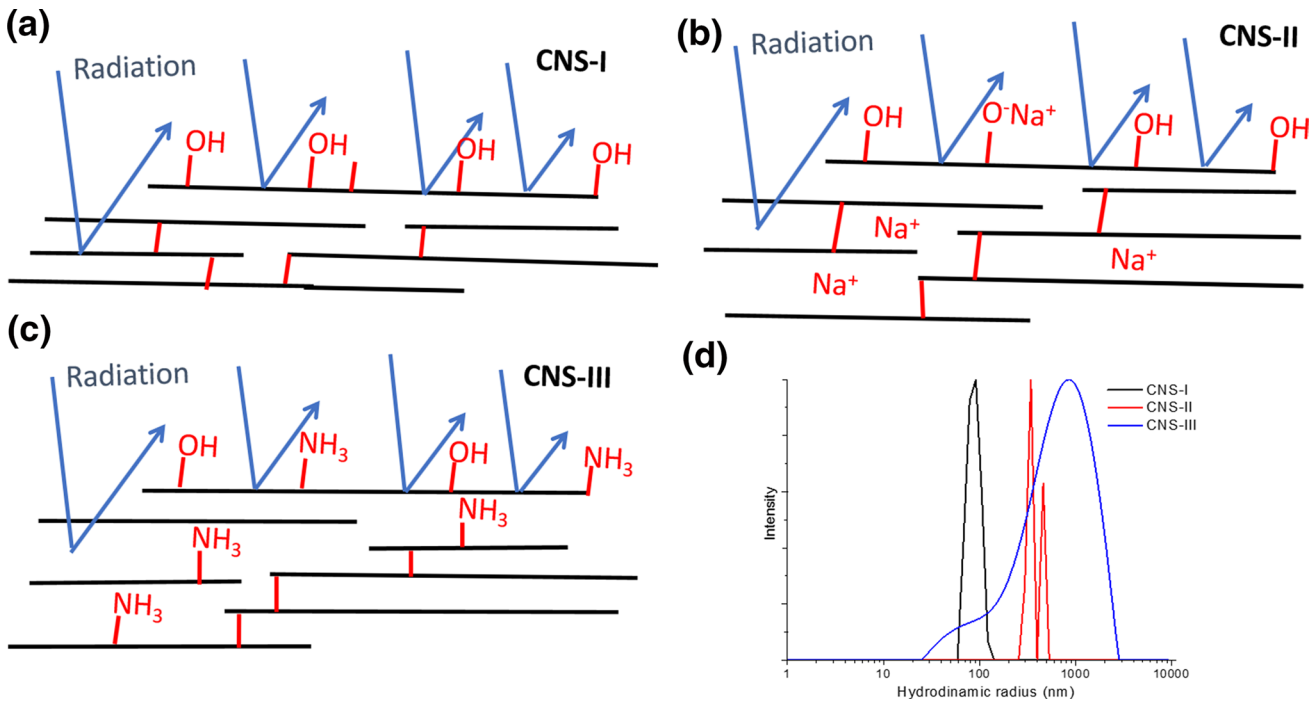

Fig. 5 Schematic representation of the surface and the atoms observed by XPS analysis of **a** CNS-I, **b** CNS-II and **c** CNS-III and **d** DLS-curves of all the polymorphs

CNS-III, which has a material part in the nanoscale (from 30 nm) and a peak of higher intensity at around 900 nm (micrometric scale). It is expected that the polymorphs tend to aggregate and differences in the morphology and sizes since there is a structural change in these samples.

Regarding stability, according to the zeta potential (ξ) theory, for a suspension to be considered stable, the zeta potential absolute values must be higher than 30 mV [12]. CNS-I e II are more stable in suspension, with ξ values of (-27.4 ± 8.8) and (-27.4 ± 7.0), respectively. The CNS-III has ξ values of (-25.5 ± 5.9). Considering the deviation of values, all polymorphs presented similar stability. This is an important parameter because the performance of the CNS as reinforcement in polymeric matrixes may be associated to the superficial charges since high ξ values indicate less agglomeration and greater dispersion of the material [12].

TEM images of CNS-I, CNS-II, and CNS-III are shown in Fig. 6. It is possible to see that the CNS-I showed typical morphology of cellulose nanocrystals. However, after the conversion of CNS-II and CNS-III, the morphology changed, and irregular rounded-like shapes could be observed. The CNS-II particles tend to agglomerate during the drying step, and no individual particles could be observed [26]; the significant change in the shape of the CNS is a strong indication that the polymorphs' preparation causes partial disruption of the crystalline structure, as described before. This result was described by Gong et al. (2018), that prepared the polymorphs before the CNS isolation; the NaOH treatment probably changed the degree of polymerization of the cellulose structure [26]. Another important factor that can be associated is the changes in the crystalline structure, i.e., the rearrangement of the cellulose chains in an anti-parallel conformation, and the process of swelling and regeneration (Fig. 6); this swelling process results in a gay by neighboring swollen nanoparticles (Fig. 5b).

For CNS-III the changes in the morphology are attributed to the change in the crystal structure since this conversion involves decrystallization and fragmentation of the crystals; the recrystallization results in the distortion of the cellulose crystals, and the fragmentation is the main responsible for the morphological changes. During the swelling process, the crystalline part of the cellulose is broken. According to O'Sullivan (1997), after the reaction, the cellulose–EDA complex resulted in non-uniform crystallinity [27].

The quasi-spherical nanoparticles probably were formed by the irregularity in the structures caused by the chemical conversions into cellulose II and III (as described before) and due to the self-assembled short nanoparticles via interfacial hydrogen bonds [5]. The prepared morphology could be potential candidates for biomedical applications and drug delivery or even a receptor for cells and drugs.

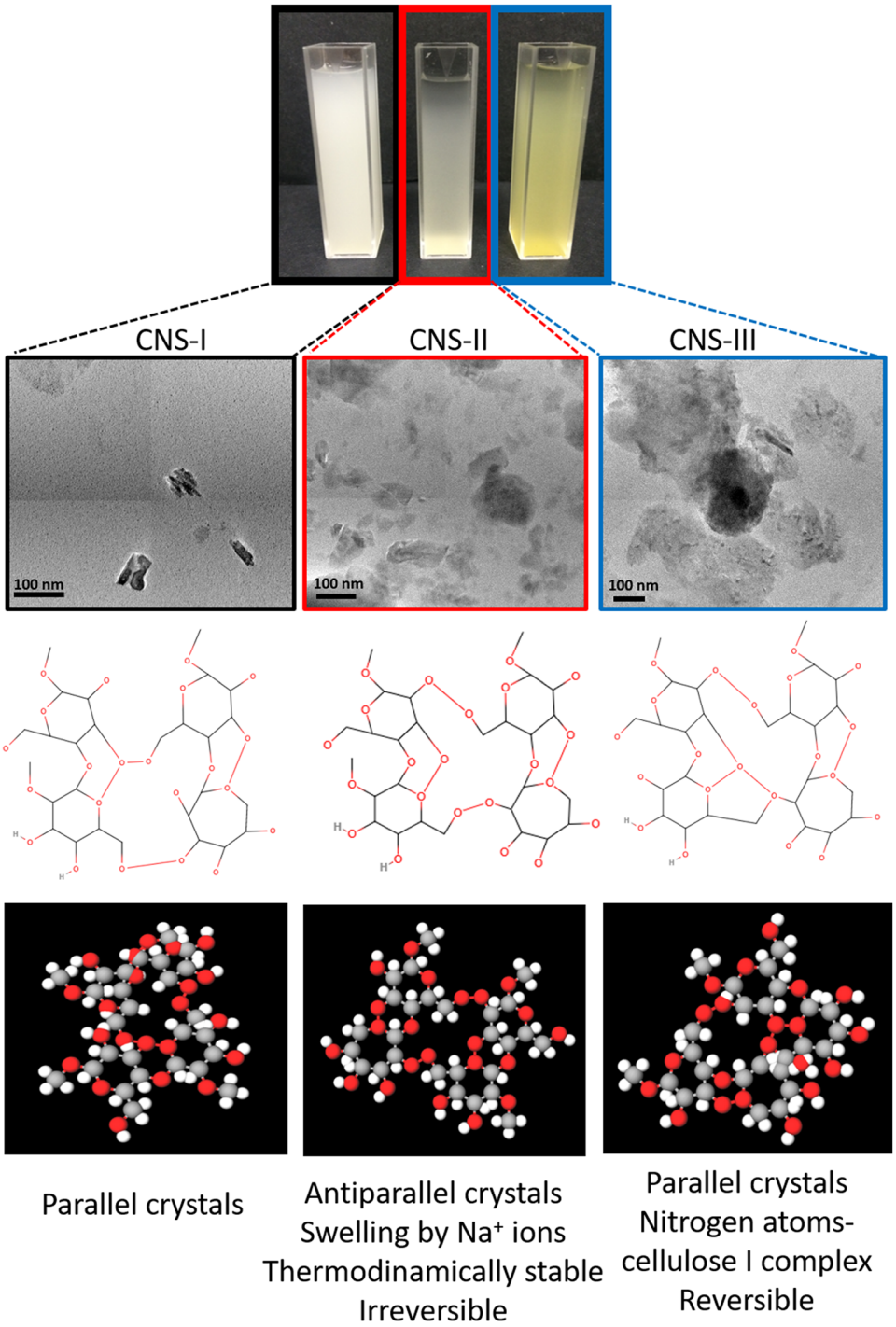

Fig. 6 Schematic representation of the CNS-I, CNS-II, and CNS-III solution, with their respective TEM images and chemical structure

Thermogravimetric Analysis (TGA)

Figure 3S represents the TGA thermograms and their derivative curves of the ER, T1, and T2 samples (Supplementary Material). Figure 7a represents the thermograms of CNS-I, CNS-II, and CNS-III and Fig. 7b their DTG curves. The CNS presents less thermal stability than the raw material; besides not having the non-cellulosic components that act as a barrier to the degradation, it can be justified by the increase of superficial area [10]. This property is important because the use of fibers and cellulose structures as polymer matrix reinforcement requires a temperature resistance since the processing occurs around 200 °C for most of thermoplastics. If the fibers degrade with the temperature, the composite may present a reduction on the mechanical properties, smell, and darkening [21].

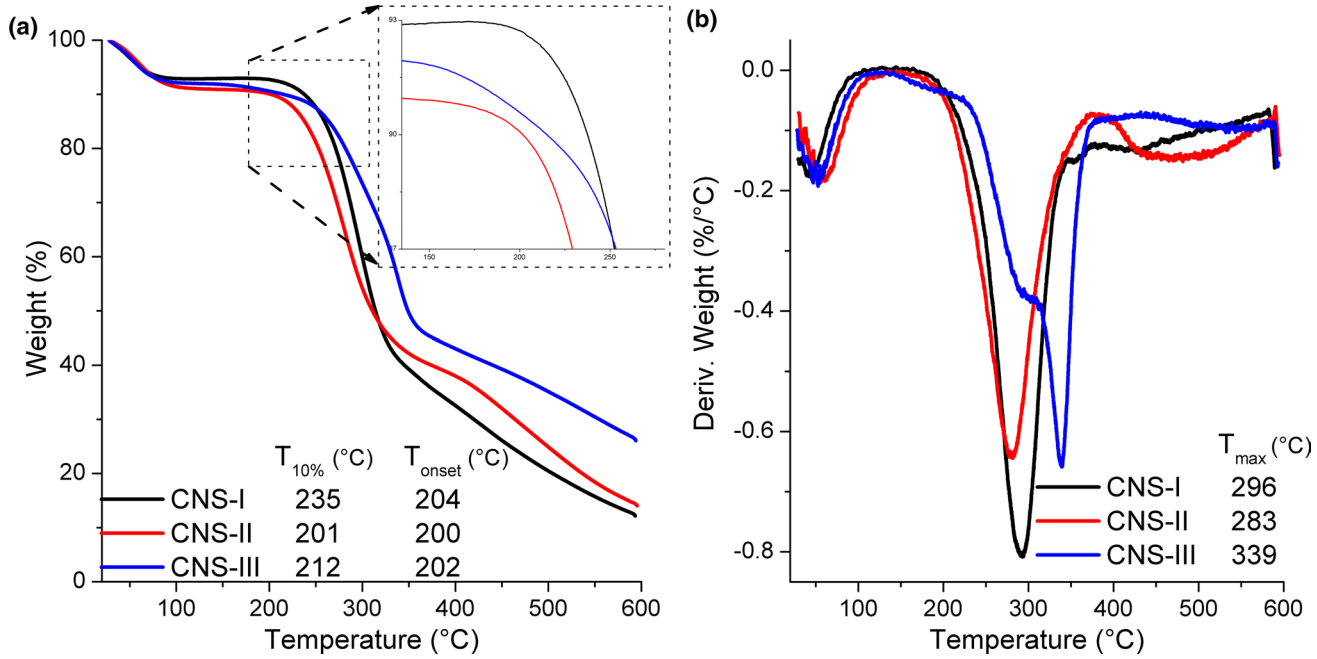

Fig. 7 **a** TGA and **b** DTG curves of CNS and their polymorphs

All the thermograms exhibit two main events of weight loss. The first one is related to the evaporation of bonded-water and occurs at 80–120 °C; the second is attributed to the cellulose thermal degradation [5]. All the CNS polymorphs have T_{onset} temperature of ~ 200 °C, which indicates good thermal properties for reinforcement, and T_{max} of ~ 295 °C. The CNS-III showed the high ashes content (~ 20%), which is probably due to the nitrogen atoms and their compounds that remained after the dialysis (as presented before). This thermal behavior allows different applications and guarantees that the CNS and their polymorphs can be applied in nanocomposites prepared by melt processing without thermal degradation.

Conclusions

In the present work, a new method was proposed to prepare cellulose polymorphs: the CNS firstly isolated by mechanical method (i.e., ball mill), and then were converted. The eucalyptus residue was used as raw material, providing for this underused waste a new destination with high technological value. The polymorphs were successfully prepared.

The FTIR evidenced changes in the characteristic spectrum of the different polymorphs. The diffraction patterns confirmed the conversion to types II and III cellulose, with both polymorphs showing lower crystallinity than type I cellulose; this may be related to the strong reagents used for the change in the crystalline structure of the samples, which results in a swelling, increased chain spacing, and structural disorganization. These changes could be confirmed by the XPS and the change in the morphology of the samples: while the cellulose I is crystalline, CNS-II and CNS-III presented irregular and quasi-spherical shapes; besides, a relation with the polymorphic transformation process was presented. All polymorphs presented good thermal stability, with potential for applications involving high temperatures.

The structural, morphological, and physicochemical variations observed among the polymorphs increase their applicability. While CNS-I is more crystalline and organized, which is desirable for the preparation of nanocomposites with high mechanical properties, the morphology and more amorphous character of CNS-II and CNS-III makes them applicable in biomedical applications, drug delivery or food.

Acknowledgements The authors thank the financial support provided by FAPESP (2018/11277-7, 22035-4 and 2018/25239-0), CNPq, CAPES, NSF-CREST #1735971, and the Multiuser Experimental Center of the Federal University of ABC (CEM-UFABC).

References

1. Kunaver M, Anžlovar A, Žagar E (2016) The fast and effective isolation of nanocellulose from selected cellulosic feedstocks. Carbohydr Polym 148:251–258. https://doi.org/10.1016/j.carbpol.2016.04.076
2. Corcelli F, Ripa M, Ulgiati S (2018) Efficiency and sustainability indicators for papermaking from virgin pulp—an emergy-based case study. Resour Conserv Recycl 131:313–328. https://doi.org/10.1016/j.resconrec.2017.11.028

3. da Silva CG, Kano FS, Rosa DS (2019) Lignocellulosic nanofiber from eucalyptus waste by a green process and their influence in bionanocomposites. Waste Biomass Valoriz.https://doi.org/10.1007/s12649-019-00610-3
4. Dufresne A (2017) Nanocellulose: from nature to high performance tailored materials, 2nd ed. De Gruyter, Berlin
5. Mahmud MM, Perveen A, Jahan RA et al (2019) Preparation of different polymorphs of cellulose from different acid hydrolysis medium. Int J Biol Macromol 130:969–976. https://doi.org/10.1016/j.ijbiomac.2019.03.027
6. Newman RH (2008) Simulation of X-ray diffractograms relevant to the purported polymorphs cellulose IVI and IVII. Cellulose 15:769–778. https://doi.org/10.1007/s10570-008-9225-5
7. Arvidsson R, Nguyen D, Svanström M (2015) Life cycle assessment of cellulose nanofibrils production by mechanical treatment and two different pretreatment processes. Environ Sci Technol 49:6881–6890. https://doi.org/10.1021/acs.est.5b00888
8. Malladi R, Nagalakshmaiah M, Robert M, Elkoun S (2018) Importance of agriculture and industrial waste in the field of nano cellulose and its recent industrial developments: a review. ACS Sustain Chem Eng.https://doi.org/10.1021/acssuschemeng.7b03437
9. Sánchez R, Espinosa E, Domínguez-Robles J et al (2016) Isolation and characterization of lignocellulose nanofibers from different wheat straw pulps. Int J Biol Macromol 92:1025–1033
10. De Souza AG, Kano FS, Bonvent JJ, Rosa DS (2017) Cellulose nanostructures obtained from waste paper industry: a comparison of acid and mechanical isolation methods. Mater Res 20:1–6
11. Gong J, Mo L, Li J (2018) A comparative study on the preparation and characterization of cellulose nanocrystals with various polymorphs. Carbohydr Polym 195:18–28. https://doi.org/10.1016/j.carbpol.2018.04.039
12. Naduparambath S, Jinitha TV, Vakyath S et al (2018) Isolation and characterisation of cellulose nanocrystals from sago seed shells. Carbohydr Polym 180:13–20. https://doi.org/10.1016/j.carbpol.2017.09.088
13. SaifulAzry SOA, Chuah TG, Paridah MT et al (2017) Effects of polymorph transformation via mercerisation on microcrystalline cellulose fibres and isolation of nanocrystalline cellulose fibres. Pertanika J Sci Technol 25:1275–1290
14. Sèbe G, Ham-Pichavant F, Ibarboure E et al (2012) Supramolecular structure characterization of cellulose II nanowhiskers produced by acid hydrolysis of cellulose I substrates. Biomacromolecules 13:570–578. https://doi.org/10.1021/bm201777j
15. Ciolacu D, Ciolacu F, Popa VI (2011) Blowoff scaling of bluff body stabilized flames. Cellul Chem Technol 45:13–21
16. Isogai A, Usuda M (1990) Crystallinity indexes of cellulosic materials. Sen'i Gakkaishi 46:324–329. https://doi.org/10.2115/fiber.46.8_324
17. Segal L, Creely JJ, Martin AE, Conrad CM (1959) An empirical method for estimating the degree of crystallinity of native cellulose using the X-ray diffractometer. Text Res J 29:786–794. https://doi.org/10.1177/004051755902901003
18. Mendes CVT, Cruz CHG, Reis DFN et al (2016) Integrated bioconversion of pulp and paper primary sludge to second generation bioethanol using *Saccharomyces cerevisiae* ATCC 26602. Bioresour Technol 220:161–167. https://doi.org/10.1016/j.biortech.2016.07.140
19. Yue Y, Han J, Han G et al (2015) Cellulose fibers isolated from energy cane bagasse using alkaline and sodium chlorite treatments: structural, chemical and thermal properties. Ind Crops Prod 76:355–363. https://doi.org/10.1016/j.indcrop.2015.07.006
20. Kim SH, Lee CM, Kafle K (2013) Characterization of crystalline cellulose in biomass: basic principles, applications, and limitations of XRD, NMR, IR, Raman, and SFG. Korean J Chem Eng 30:2127–2141. https://doi.org/10.1007/s11814-013-0162-0
21. Poletto M, Júnior HLO, Zattera AJ (2014) Native cellulose: structure, characterization and thermal properties. Materials (Basel) 7:6105–6119. https://doi.org/10.3390/ma7096105
22. García A, Labidi J, Belgacem MN, Bras J (2017) The nanocellulose biorefinery: woody versus herbaceous agricultural wastes for NCC production. Cellulose 24:693–704. https://doi.org/10.1007/s10570-016-1144-2
23. Nelson ML, O'Connor RT (1964) Relation of certain infrared bands to cellulose crystallinity and crystal lattice type. Part II. A new infrared ratio for estimation of crystallinity in celluloses I and II. J Appl Polym Sci 8:1325–1341. https://doi.org/10.1002/app.1964.070080323
24. Qin L, Li WC, Zhu JQ et al (2015) Ethylenediamine pretreatment changes cellulose allomorph and lignin structure of lignocellulose at ambient pressure. Biotechnol Biofuels 8:1–15. https://doi.org/10.1186/s13068-015-0359-z
25. Sawada D, Hanson L, Wada M et al (2014) The initial structure of cellulose during ammonia pretreatment. Cellulose 21:1117–1126. https://doi.org/10.1007/s10570-014-0218-2
26. Li X, Li J, Gong J et al (2018) Cellulose nanocrystals (CNCs) with different crystalline allomorph for oil in water Pickering emulsions. Carbohydr Polym 183:303–310. https://doi.org/10.1016/j.carbpol.2017.12.085
27. O'Sullvian AC (1997) Cellulose: the structure slowly unravels. Cellulose 4:173–207